© 2024. Published by The Company of Biologists Ltd | Journal of Experimental Biology (2024) 227, jeb246840. doi:10.1242/jeb.246840

RESEARCH ARTICLE

Flight power muscles have a coordinated, causal role in controlling hawkmoth pitch turns

Leo J. Wood[1,2], Joy Putney[1,3] and Simon Sponberg[1,2,3,*]

ABSTRACT

Flying insects solve a daunting control problem of generating a patterned and precise motor program to stay airborne and generate agile maneuvers. In this motor program, each muscle encodes information about movement in precise spike timing down to the millisecond scale. Whereas individual muscles share information about movement, we do not know whether they have separable effects on an animal's motion, or whether muscles functionally interact such that the effects of any muscle's timing depend heavily on the state of the entire musculature. To answer these questions, we performed spike-resolution electromyography and electrical stimulation in the hawkmoth *Manduca sexta* during tethered flapping. We specifically explored how flight power muscles contribute to pitch control. Combining correlational study of visually induced turns with causal manipulation of spike timing, we discovered likely coordination patterns for pitch turns, and investigated whether these patterns can drive pitch control. We observed significant timing change of the main downstroke muscles, the dorsolongitudinal muscles (DLMs), associated with pitch turns. Causally inducing this timing change in the DLMs with electrical stimulation produced a consistent, mechanically relevant feature in pitch torque, establishing that power muscles in *M. sexta* have a control role in pitch. Because changes were evoked in only the DLMs, however, these pitch torque features left large unexplained variation. We found this unexplained variation indicates significant functional overlap in pitch control such that precise timing of one power muscle does not produce a precise turn, demonstrating the importance of coordination across the entire motor program for flight.

KEY WORDS: Motor control, Neuromechanics, *Manduca sexta*, Muscle coordination, Insect flight, Stimulation

INTRODUCTION

Locomoting animals have to generate a motor program, a coordinated spatial and temporal pattern of activity sent to an array of muscles to produce behaviors. Each muscle is controlled by action potentials, or spikes, which carry information about the motion of an animal to a highly precise millisecond or sub-millisecond scale (Putney et al., 2019; Sober et al., 2018). This is significant because the degree to which muscles are functionally coordinated, such that the kinematic and behavioral action of individual muscles depends on the action of other muscles, determines how precise spike timing translates to movement. If a single muscle independently controls specific features of kinematics or dynamics, then precisely timed spikes to that muscle can be directly attributed to precise behavioral outcomes. But if control is orchestrated across many muscles simultaneously such that the action of one muscle changes the potential of another muscle to perform control, then the transformation of a precise change in spike timing into movement will depend on the context created by the spiking patterns in the rest of the motor program. Such a dependency might be expected as muscles often act in coordinated groups (Ting, 2007), produce context-dependent mapping between bulk muscle activation and kinematics (Kutch and Valero-Cuevas, 2011; Valero-Cuevas, 2009) and can share information even at the level of individual spikes (Putney et al., 2019). But does this shared information translate into functional coordination, or do individual muscles have separable, independent effects on behavioral outcomes?

Insect flight provides a particularly tractable system for studying this question. While flight is a complex, 3D form of locomotion, in many orders of flying insects such as Diptera and Lepidoptera, as few as 12 muscles – all effectively single motor units (Rheuben, 1985; Usherwood, 1962) – generate all of the motion and control of the wings (Lindsay et al., 2017; Putney et al., 2019). This motor program is separated into indirect flight muscles and a set of steering muscles that directly attach to the wing, all contained within the thorax of the body. Two large pairs of flight power muscles, the dorsolongitudinal muscles (DLMs) and dorsoventral muscles (DVMs), produce most of the mechanical power for flight, while smaller steering muscles directly deform the wing hinge to adjust wing kinematics (Eaton et al., 1988). Steering muscles are well known to perform flight control, with timing of individual muscles often correlated to specific maneuvers and wing kinematics (Ando and Kanzaki, 2004; Balint and Dickinson, 2004; Dickinson and Tu, 1997; Hedenström, 2014; Lindsay et al., 2017; Melis et al., 2024; Sadaf et al., 2015; Tu and Dickinson, 1996; Wang et al., 2008; Whitehead et al., 2022). However, in larger synchronous insects such as the hawkmoth *Manduca sexta*, the time scale of power muscle force production is well within a single wingstroke (Tu and Daniel, 2004), providing a clear case where both power and steering muscles are actively involved in flight control (Ando and Kanzaki, 2016; Sponberg and Daniel, 2012; Sponberg et al., 2015a). Hawkmoths generally provide an excellent window into muscle coordination, especially through the lens of spike timing, as a comprehensive flight motor program can be recorded to a spike-level resolution in a behaving animal, simultaneous with time-resolved body forces and torques (Putney et al., 2019).

In hawkmoths, then, is the motor program functionally coordinated? The hawkmoth flight motor program is known to

[1]Quantitative Biosciences Program, Georgia Institute of Technology, Atlanta, GA 30313, USA. [2]School of Physics, Georgia Institute of Technology, Atlanta, GA 30313, USA. [3]School of Biological Sciences, Georgia Institute of Technology, Atlanta, GA 30313, USA.

*Author for correspondence (sponberg@gatech.edu)

L.J.W., 0000-0003-1829-7781; J.P., 0000-0002-8736-4282; S.S., 0000-0003-4942-4894

Received 8 November 2023; Accepted 14 October 2024

be submillisecond precise (Putney et al., 2019, 2023b), and correlational evidence suggests a high degree of coordination and overlapping control potentials. In an information-theoretic sense, the hawkmoth flight motor program is coordinated so that spike timing of all muscles carries redundant global information about behavioral output (Putney et al., 2019). Linear combinations of muscle activity also explain the behavioral output of multiple different turning maneuvers, allowing 90% accurate decoding of the type of turn maneuver performed from the activity of at minimum only four muscles (Putney et al., 2021 preprint). In some functionally coordinated systems, linear combinations of commands across multiple muscles called muscle synergies can describe the majority (often >90%) of output variation (Ting, 2007). However, yaw turning behaviors in hawkmoths were better described by the independent activity of muscles than as a synergy (Sponberg et al., 2015a). These lines of evidence are mixed, suggesting that muscles in the hawkmoth flight motor program have overlapping control potentials, but also have potentially independent effects on an animal's motion.

A major driver of this conflicting picture is that when the spike timing of many muscles may be correlated with behavior, it is challenging to separate the causal contributions of individual muscles to a given behavioral output. Direct electrical stimulation of muscles and motor neurons can reveal a muscle's control potential, by causally inducing specific spike timing in specific situations. As an *in vivo* manipulation of muscle activity, electrical stimulation has been used to identify muscle control potentials in anesthetized vertebrates (Vazquez, 1995), elicit control changes in flying insects via high-frequency stimulation (Sato and Maharbiz, 2010; Sato et al., 2015) or perform bulk perturbation to specific sides of an insect (Tsang et al., 2010). More rarely, however, it has been applied in behaving invertebrates to produce targeted, spike-level manipulations of specific muscle timings (Sponberg et al., 2011). In hawkmoths, altering motoneuron spike timing shows a causal connection between left–right timing differences in primary downstroke muscles and yaw torque (Sponberg and Daniel, 2012). However, for flying insects, these temporally precise manipulations and related correlational studies have only focused on left–right asymmetries leading to roll or yaw turns (Fernández et al., 2012; Sponberg and Daniel, 2012; Sponberg et al., 2015a; Springthorpe et al., 2012; Wang et al., 2008). Causal manipulation of steering muscles to produce pitch turns has been performed in fruit flies using optogenetics (Whitehead et al., 2022), but for flying insects no spike-level manipulations have been performed to study pitch turns.

Gaps such as these are notable because pitch turns are particularly interesting for hovering insects. Nearly every model of insect flight dynamics identifies an unstable mode resulting from coupled oscillations in fore–aft velocity and pitch, requiring some degree of active neuromuscular control (Kim and Han, 2014; Kim et al., 2015; Ristroph et al., 2013; Windsor et al., 2014). Active control of pitch must also be bilaterally symmetric by nature, so any control cannot simply result from left–right motor program asymmetries (Jankauski et al., 2017). Though flying insects such as dipterans and lepidopterans control pitch through a multifaceted set of passive and active mechanisms, including passive vibrational stability via wing oscillation (Taha et al., 2020) and movement of the center of mass (COM) relative to the center of pressure (COP) via abdominal motion (Frye, 2001; Hedrick and Daniel, 2006; Hinterwirth and Daniel, 2010; Le et al., 2023; Ristroph et al., 2013), most pitch control is thought to arise from the activity of the steering muscles (Whitehead et al., 2015, 2022). While modulation of spike timing in the flight power muscles has been closely linked to roll and yaw turns (Lehmann et al., 2013; Sponberg and Daniel, 2012; Sponberg et al., 2015a; Springthorpe et al., 2012), it is not known to what degree power muscles can also control pitch turns. Such turns require not left–right phase separation but modulation of kinematics between the downstroke and upstroke. If the indirect power muscles are capable of contributing to pitch control, they must do so through alteration of wing kinematics, either moving the COP, changing time-varying wing forces, or producing inertial moments on the COM. In freely flying hawkmoths, pitching up in response to looming stimuli correlates with changes in angle of attack, stroke plane tilt, angle at wingstroke reversals and deviation angle at wingstroke reversals (Cheng et al., 2011). The interval between the DLM and DVM has been implicated in changing deviation angle of the wing in free flight (Wang et al., 2008), and shown to change with flight speed in forward flight, so may be related to modulating power production (Hedrick et al., 2017).

Overall, however, while the precise spike timing of the hawkmoth power muscles has been connected to asymmetric kinematics, their potential for control of other maneuvers such as pitch turns is unclear. We hypothesized that the indirect power musculature in the hawkmoth *Manduca sexta* does contribute to pitch control. We also hypothesized that the flight motor program is functionally coordinated, such that even the mapping of individual action potentials of large power muscles into movement (the muscle's control potential) (Sponberg et al., 2011) is dependent on the context of the rest of the motor program. Alternatively, we might see that the flight motor program is not very functionally coordinated, so that the control potentials of individual muscles are easily identified and not affected by the activity of other muscles. Using a combination of correlational and causal experiments, we tested both of these hypotheses, identifying an association between power muscle activity and pitch turns, then rewriting motor activity to reproduce those patterns in tethered flight.

MATERIALS AND METHODS

Animals

All moths, *Manduca sexta* (Linnaeus 1763), were obtained as pupae and housed communally after eclosion with a 12 h:12 h light:dark cycle (N=9, University of Washington colony and Carolina Biological Supply Co. for visually induced turning experiments; N=5, Case Western Reserve colony for stimulation experiments). Naive males and females were used in experiments conducted during the dark period of their cycle. EMG recordings were performed on cold-anesthetized moths by inserting pairs of silver wire [diameter 0.005 inch (0.127 mm)] into the thorax and fastening them with cyanoacrylate glue, following the same procedure as Putney et al. (2019). After wire insertion, moths were fastened with cyanoacrylate glue to a tether rigidly attached to a custom six-axis load cell (ATI Nano17ti, FT20157; calibrated ranges F_x,F_y=±1.0 N, F_z=±1.8 N, τ_x,τ_y,τ_z=±6.25 mN m). After attachment, moths were left to dark adapt for 30 min at luminance levels typical for when these crepuscular moths are active (Sponberg et al., 2015b).

High-amplitude optomotor turns in visual arena experiments

The data of constant high-amplitude optomotor-induced turns were originally published by Putney et al. (2021 preprint). Moths were presented with wide-field sinusoidal gratings on a rendered 3D sphere in Microsoft Visual Studio (Fig. 1). The stimuli were projected onto three computer monitors (ASUS PG279Q ROG Swift; 2560×1440 pixels) overlaid with neutral density filters to obtain peak sensitivity luminance conditions for *M. sexta* of

Journal of Experimental Biology (2024) 227, jeb246840. doi:10.1242/jeb.246840

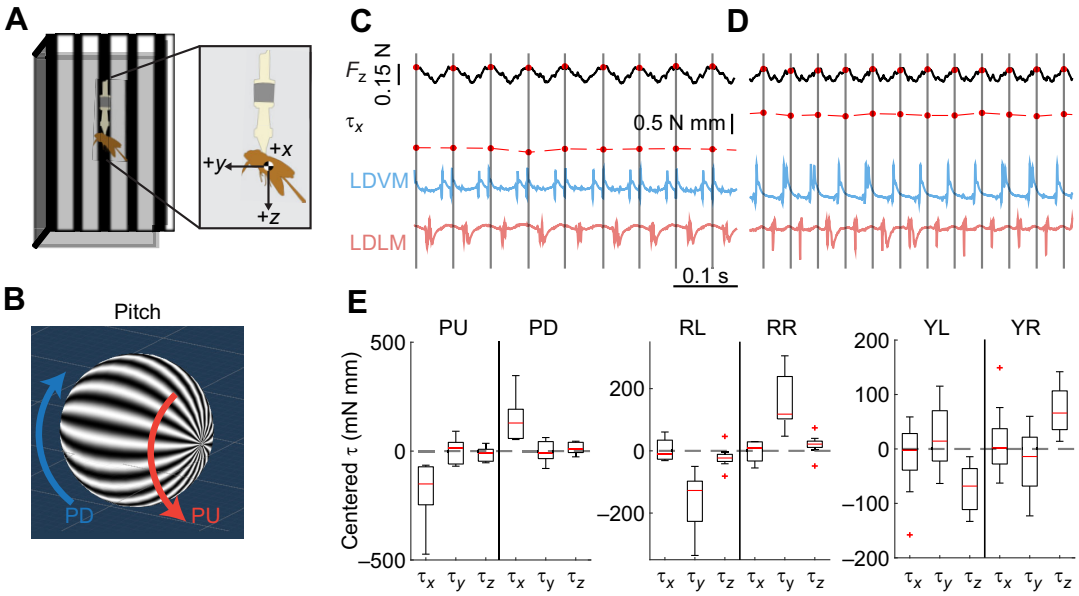

Fig. 1. Constant high-amplitude optomotor turns produce separated body torque responses. Tethered moths were shown three pairs of visual stimuli to elicit high-amplitude turns about the three flight axes – pitch, roll and yaw. (A) Schematic diagram of the visual stimulus arena formed by three computer monitors, with the moth tethered in the center. Inset depicts the coordinate frame used throughout. (B) Example of wide-field stimuli in pitch direction. Widefield sinusoidal gratings on a projected 3D sphere, with spheres rotated with a constant drift velocity produce two different stimulus conditions for each axis of rotation. PD, pitch down; PU, pitch up. (C,D) Simultaneous raw EMG recordings of the left side power muscles with motor output for 0.5 s in the pitch up (C) and pitch down (D) conditions. Wingstrokes were segmented using the Hilbert transform of F_z force. Wingstroke-averaged pitch torque (τ_x) demonstrates different behavior in response to the visual stimulus conditions. LDVM, left dorsoventral muscle; LDLM, left dorsolongitudinal muscle. (E) Centered mean wingstroke-averaged pitch (τ_x), roll (τ_y) and yaw (τ_z) torques for each individual moth (N=9) in six conditions: PU, PD, roll left (RL), roll right (RR), yaw left (YL) and yaw right (YR). Boxplots report the mean across individuals (red line), the 25th and 75th percentiles (box region), and the total range (whiskers) excluding outliers (red crosses).

approximately 1 cd m^{-2} (Stöckl et al., 2017). The tethering set-up placed the moth at the center of a three-sided box formed by these three monitors (Fig. 1A). The sinusoidal gratings had a spatial frequency of 20 deg cycle^{-1}, and the sphere was rotated to place its axis of rotation along each of the Earth-coordinate system flight axes of pitch, roll and yaw (Fig. 1B). The sphere was then rotated about this axis in opposite directions at a constant drift velocity of 100 deg s^{-1} (5 cycles s^{-1}), which was chosen as this spatiotemporal frequency drove high responses in the moth visual system (Stöckl et al., 2017). Therefore, each moth responded to six distinct visual stimulus conditions, three pairs about each flight axis: pitch up, pitch down, roll left, roll right, yaw left and yaw right.

Simultaneous strain gauge voltage recordings from the F/T transducer and EMG recordings from the silver wire electrodes were taken as the moth responded to each of the six stimulus conditions for 20 s, each recorded at 10 kHz. The strain gauge voltages were converted to the three forces and three torques on each axis at the estimated average COM for tethered moths. These forces and torques were lowpass filtered using an 8th order Butterworth filter with a cutoff of 1000 Hz. To segment wing strokes in some analyses, a type II Chebyshev filter was applied to F_z with a bandpass between 5 and 35 Hz to capture the range of wingbeat frequencies observed in this dataset (15–27 Hz). The Hilbert transform of this filtered signal was taken to estimate the wingstroke phase, and individual wingstrokes were separated by finding negative-to-positive zero crossings of this phase, with t=0 for each wingstroke occurring at these crossings. This use of the Hilbert transform to find instantaneous phase and separate a gait into specific cycles has previously been used in hawkmoths (Putney et al., 2019; Sponberg et al., 2015a), gait analysis of cockroaches (Revzen and Guckenheimer, 2008) and rat whisking (Hill et al., 2011). Spikes in the raw EMG voltage recordings were discriminated using Offline Sorter (OFS; Plexon) via threshold crossing. Where necessary, filtering options in this software were used to correct baseline wander, motion artifacts and other noise that made discriminating spikes difficult. Spike times were specified to 0.1 ms relative to zero phase in each wing stroke as described above.

Centered wingstroke mean torques were used to compare between opposing conditions in pitch, roll and yaw (Fig. 1E). Centering was performed by subtracting from per-wingstroke mean pitch, roll and yaw torques the per-moth overall mean pitch, roll and yaw torques τ_x, τ_y and τ_z across all that moth's data for both conditions (i.e. both pitch up and pitch down turns). Centering was performed independently for each moth (N=9 moths).

Electrical stimulation experiments

To causally manipulate power muscle timing and observe resulting changes in flight forces and torques, electrical stimulation was used to alter the spike timing of the DLMs. While there are many previous studies eliciting control changes in flying insects using high-frequency electrical stimulation (Sato and Maharbiz, 2010; Sato et al., 2015) or bulk stimulation of individual sides of an insect (Tsang et al., 2010), here we used targeted and precisely timed stimulation to induce single action potentials in the DLMs, in a method more akin to that of Sponberg and Daniel (2012) and Sponberg et al. (2011).

Moths attached to a six-axis load cell tether would freely engage in bouts of flapping flight, during which the DLMs would be stimulated with a specific timing relative to the DVMs. Stimulus delay times were chosen at random from a range of 4 to 40 ms after DVM spike detection, with each delay time applied for a 20 s recording period with EMG and F/T transducer recorded at 10 kHz.

Journal of Experimental Biology (2024) 227, jeb246840. doi:10.1242/jeb.246840

Single 0.25 ms pulses of either constant current or constant voltage were applied to silver wires placed on either end of each DLM, with each stimulation separated by at least 4 s to avoid entrainment. A diagram signal flow used for stimulation is shown in Fig. 2A. In brief, timing of the stimulus was achieved by passing either the left or right DVM voltage recording through a custom analog spike-detection circuit and microcontroller. The controller would trigger a stimulator (A-M Systems Model 3800) with a stimulus isolation unit (A-M Systems Model 2200) on a controlled delay time from the onset of a detected DVM spike.

All stimulus pulses were biphasic, but specific stimulus features were calibrated for each moth individually, such as whether constant current or voltage was used and of what amplitude. This calibration in an example moth is shown in Fig. 2B. The stimulus was repeatedly applied while the moth was in a quiescent state, with stimulation amplitude steadily increased until evoked motor action potentials were observed in both DLMs with no evoked action potentials observed in surrounding muscles (Fig. 2B). While most individuals had their best response from constant-current stimulation, differences in electrode placement and individual anatomy and physiology resulted in better results for some individuals from constant-voltage stimulation. After calibration, stimuli ranged from 0.05 to 0.1 mA for constant-current stimulation and from 5 to 10 V for constant voltage. Note that, as shown in Fig. 2B, evoked action potentials occur roughly 4 ms after a pulse of current is applied.

Spike discrimination, wingstroke segmentation and FT data calibration and filtering followed the same parameters as described previously (Putney et al., 2019), with several exceptions. As the load cell the moth is tethered to measure forces and torques at a distance from the moth's actual COM (which is typically between the thorax and the first abdominal segment), strain gauge voltages had to be transformed to COM locations estimated for each individual. This estimation was performed using bounded linear least-squares minimization to find the COM location which minimized torques to zero during fully quiescent data of each tethered moth. Different filter parameters were used for wingstroke segmentation, specifically a 4th order type II Chebyshev filter with a 10–40 Hz

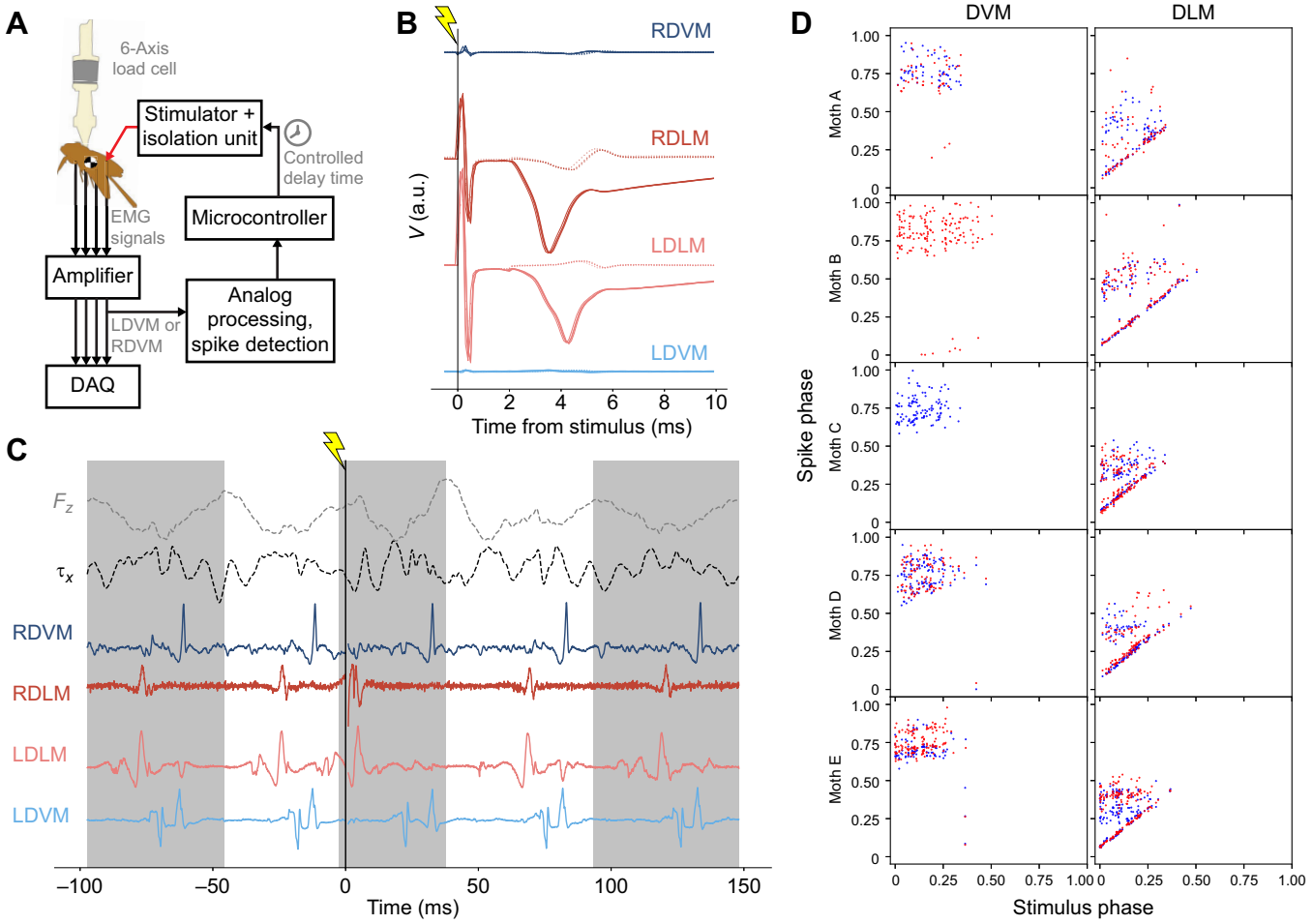

Fig. 2. Electrical stimulation allows controlled change of DLM timing, leading to changes in body pitch torque. (A) Diagram of stimulation experiment signal flow. Analog spike detection is run on a DVM signal post-amplification, enabling a microcontroller to trigger a stimulator with specific timings relative to observed DVM spikes (see Sponberg and Daniel, 2012, for a similar experiment). (B) Voltage recordings, aligned at the time of the stimulus, from all four power muscles in a quiescent moth while stimulation is applied, illustrating the efficacy of electrical stimulation. Lighter dotted traces are 0.03 mA current of stimulation, darker solid traces are 0.05 mA current. (C) Example trace of EMG and vertical force (F_z) and pitching torque data (τ_x) during stimulation. Stimulation was applied at time t=0 (denoted by vertical line with lightning symbol) and produced a phase advance in right and left DLM (RDLM and LDLM) spikes. Alternating shaded regions indicate wingstrokes found via negative-to-positive zero crossings of the Hilbert transform of F_z (light gray dashed line). (D) Phase of all spikes in stimulation wingstroke plotted against the phase at which stimulation was applied for that wingstroke on the x-axis. Red points indicate right muscle, blue points indicate left muscle. If stimulation is inducing spikes in the DLM, then spikes along an identity line should be observed only in the DLM (right) column. Note that mean natural DLM phase of this dataset is at 32.7% of the wingstroke.

passband, as this demonstrated better wingstroke segmentation performance for the stimulation data.

Stimulation trials were included in this study only if the stimulus evoked a muscle action potential (MAP) in both DLMs, and if the first observed MAP from both DLMs in the stimulus wingstroke was evoked rather than natural. MAPs were deemed evoked rather than natural if they occurred within a 5 ms window directly following stimulation. Fig. 2D provides a visual aide for how evoked MAPs were selected; wingstrokes were only included if both left and right DLMs had a MAP occur along the main diagonal of Fig. 2D, and if the first spike in the stimulation wingstroke occurred along this diagonal.

Feature extraction and stimulation analysis

To analyze the effects of controlled DLM timing on pitch torque, features of pitch torque which were associated with evoked DLM timing had to be extracted and quantified. To extract features of pitch torque that correlated with stimulation-evoked changes in DLM timing, canonical correlation analysis (CCA) was employed with the cross-decomposition module of the *scikit-learn* python package (Pedregosa et al., 2011), which utilizes a previously described algorithm (Wegelin, 2000). CCA is one of several dual-dimensionality reduction methods, such as partial least squares regression (PLS) (Sponberg et al., 2015a; Wegelin, 2000), where two sets of latent variables (or 'features') T' and Y' which maximally correlate with each other are extracted from two sets of original data variables T and Y. CCA is very closely related to the commonly used principal components analysis (PCA) in that it uses an eigendecomposition to construct components (or 'features') from a linear combination of variables in a dataset. In PCA, these features are constructed to maximize variance, whereas in CCA and the broader family of PLS, two sets of features which maximally correlate with each other are constructed simultaneously from two sets of variables. By inputting the set of pitch torque waveforms for T and the stimulation-evoked DLM timing or phase for T, we can extract a feature of the pitch torque data, T', which maximally correlates with evoked timing changes.

CCA was performed on each individual moth independently with pitch torque data assembled into a matrix $\mathbf{T}$ and stimulation-evoked DLM phase assembled into a matrix $\mathbf{Y}$. Pitch torques for all stimulation wingstrokes were linearly interpolated to m=300 samples long and assembled into an $n\times m$ matrix $\mathbf{T}$, where n is the number of valid stimulation wingstrokes for that individual. The other CCA input, $\mathbf{Y}$, was constructed as an $n\times k$ matrix of just a single variable, the phase of the evoked DLM spike for each stimulation wingstroke (k=1 for the duration of this paper).

Note that CCA was performed on z-scored versions of $\mathbf{T}$ and $\mathbf{Y}$, denoted throughout by caret hats as $\hat{\mathrm{T}}$ and $\hat{Y}$, respectively. z-scoring allows for more stable operation on data of different ranges and units by making variance non-dimensional and placing disparate data in similar ranges. Note that when quantities are provided in real units z-scoring is inverted.

For $\mathbf{T}$ and $\mathbf{Y}$, CCA produces a $k\times m$ set of features often referred to as 'loadings', $\mathbf{T}_{\text{loadings}}$, an $m\times k$ set of 'weights' used to construct the features, $\mathbf{T}_{\text{weights}}$, and an $n\times k$ set of 'scores' defined by $\mathbf{TT}_{\text{weights}}$, effectively the projection of the data in $\mathbf{T}$ to the reduced set of features T'. Data in $\mathbf{T}$ can be reconstructed from the features in $\mathbf{T}_{\text{loadings}}$:

$$\hat{\mathbf{R}} = \mathbf{T}_{\text{scores}}\mathbf{T}_{\text{loadings}}^{T}, \tag{1}$$

where $\hat{\mathbf{R}}$ is an $n\times m$ matrix of approximations of the original data in $\mathbf{T}$ via linear scaling of the feature vector $\mathbf{T}_{\text{loadings}}$. Note that, as denoted by the caret hat, $\hat{\mathbf{R}}$ is still z-scored, and the inverse of the z-scoring is applied to obtain values with real units.

Angular impulse, or net change in angular momentum, was calculated from pitch torque of extracted features and original pitch torque data for individual wingstrokes as:

$$\Delta L = \int_{t_1}^{t_0} \tau_x \mathrm{d}t, \tag{2}$$

where t_0 and t_1 define the start and end times of the wingstroke, respectively. We obtained effective pitch angular velocity due to pitch torque as:

$$\Delta\omega = \frac{\Delta L}{I_{yy}}, \tag{3}$$

where I_{yy} is the pitch moment of inertia for *M. sexta*, defined throughout this work as I_{yy}=266.7 g mm^{-2} from Cheng et al. (2011). Numerical integration was performed with the trapezoidal method, with CCA feature reconstructions resampled from m=300 to the original number of samples present in the corresponding wingstroke.

Any testing for significant linear relationships between induced DLM timing and aggregate variables of flight mechanics, such as pitch angular impulse or wingstroke-averaged forces and torques, was performed using a linear mixed effects model in R (http://www.R-project.org/) using the *nlme* library (https://CRAN.R-project.org/package=nlme). All models were fitted with individual moth as a random intercept effect, with effect significance determined by a P<0.05 cutoff.

RESULTS

We investigated the relationship between precise spike timing of the flight power muscles in *M. sexta* and pitch turns through two main approaches. In the first experiment, n=21,203 total wingstrokes were analyzed from N=9 moths induced to perform roll, pitch and yaw turns through rotating wide-field visual stimuli to correlate how timing of the primary flight muscles changed between pitch up and pitch down turns. In the second experiment, in n=345 wingstrokes across N=5 moths, we causally manipulated the timing of the primary downstroke muscles, the DLMs, to observe changes in pitch torque due to altering the relative timing of the primary flight power muscles.

Power muscle spike timing correlates with pitch turns in visually induced turns

Mean centered torques for each condition showed separation on the expected axis (Fig. 1E), demonstrating that each condition indeed elicited a strong turn response from moths in only the desired direction. For instance, overall mean wingstroke torques per individual moths (N=9) were statistically significantly different between mean pitch torque τ_x (P=0.003 in paired t-test), but not between mean roll or yaw torques (P>0.05 in paired t-tests for τ_y and τ_z).

When moths responded to pitch conditions, the time between the DLM spike and the first DVM spike increased in duration when pitching up (Fig. 3). In absolute time, mean duration between spikes across same-side DLM–DVM pairs was significantly different between pitch up and pitch down conditions (pitch up 24.5±0.8 ms, pitch down 17.6±0.7 ms; Fig. 3A,B,E). Interestingly, wingbeat frequency was much lower in pitch up than in pitch down conditions in all moths, with a mean wingbeat frequency of 18.6±0.4 Hz in pitch up and 22.9±0.5 Hz in pitch down (Fig. 3F). This could indicate that moths lower their wingbeat frequency when executing

Journal of Experimental Biology (2024) 227, jeb246840. doi:10.1242/jeb.246840

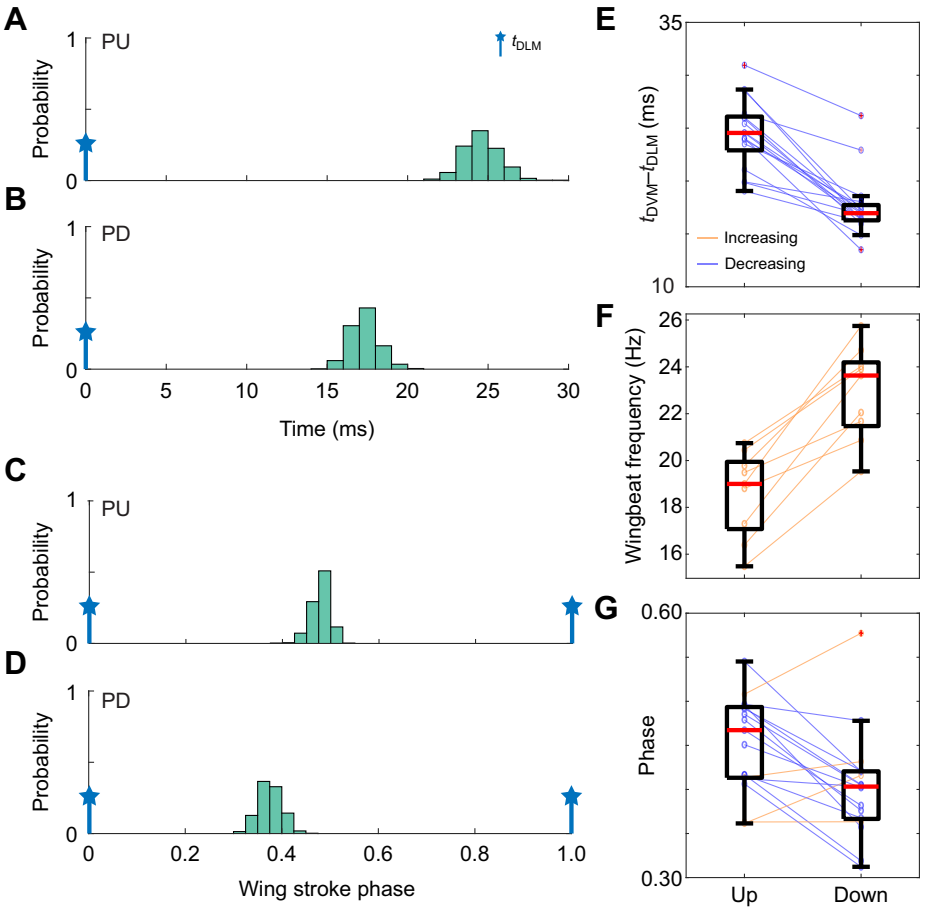

Fig. 3. Timing between the DVM and DLM muscles increases when moths pitch up. (A,B) Normalized histograms from an example moth of the first DVM spike timing in each wingstroke (t_{DVM}) with respect to the DLM timing (t_{DLM}=0) for the pitch up (A) and pitch down (B) conditions. (C,D) Normalized histograms from the same example moth of the phase of the first DVM spike in each wing stroke with respect to the DLM timing for pitch up (C) and pitch down (D). (E) Absolute timing difference between t_{DVM} and t_{DLM} for 17 same-side DLM–DVM pairs for the pitch up and pitch down conditions (N=9 moths for 19 same-side pairs, with one failed DVM recording eliminating a pair). Means are statistically different ($P<10^{-6}$ for paired t-test). (F) Wingbeat frequency for all 9 moths for the pitch up and pitch down conditions (means statistically different, $P<10^{-3}$ for paired t-test). (G) Phase of the first DVM spike in each wingstroke with respect to the DLM timing for 17 same-side DLM–DVM pairs (means statistically different, P=0.003 for paired t-test). Boxplots report the mean across individuals (red line), the 25th and 75th percentiles (box region), and the total range (whiskers) excluding outliers (red crosses).

pitch up maneuvers. Because there is a change in wingbeat period between pitch up and pitch down conditions of ∼10.1 ms, which could account for the observed difference in t_{DVM}–t_{DLM} in absolute time, we normalized t_{DVM}–t_{DLM} to the length of each wingstroke (Fig. 3C,D,G). Mean phase between same-side DLM–DVM pairs was 45±1% of the wingstroke in pitch up conditions and 40±1% in pitch down conditions, with the majority of individuals showing this trend (Fig. 3G).

Together, these results demonstrate a correlation between DLM and DVM timing and pitch turns: in pitch up, the time between DLM and DVM spikes is greater, and in pitch down the time is reduced. While these data do not implicate any specific mechanisms or causal links between this timing shift and pitch turning, the high consistency of the observed timing shift suggests a functional role played by the power muscles in controlling pitch turns.

Altered DLM timing produces consistent changes to within-wingstroke pitch torque dynamics

Tuned, brief electrical stimulation can elicit MAPs in both of the main downstroke muscles of *M. sexta* without cross-stimulation of other muscles (Fig. 2B), including in tethered flapping when all flight muscles are highly active (Fig. 2C,D). Beyond simply inducing spikes, this method of electrical stimulation can perform a ‘motor overwrite’, fully preventing natural spikes from occurring in their normal timing, if the natural spikes are suppressed by the refractory period of the motor unit (Sponberg and Daniel, 2012). This is seen both in the provided example trace, where only single spikes shifted earlier than their natural timing are observed in the stimulation wingstroke for both DLMs (Fig. 2C), and more generally in the complete data of spike times where stimulation applied in the 0.2–0.4 phase range visibly offsets or eliminates other spikes in the stimulation wingstroke (Fig. 2D). Causally manipulating DLM timing in single wingstrokes produced consistent and observable effects on within-wingstroke pitch torque (Fig. 4). When pitch torque traces were binned into groups by stimulation phase, pitch torque deviated from pre-stimulus wingstrokes (Fig. 4A,B). Typical wingstrokes had a 3- or 4-cycle oscillation in pitch torque, which matches robotic flapping models of *Manduca* (Cheng et al., 2011), but evoked DLM spikes shifted the phase of these torque oscillations. Note that for all individuals, immediately after stimulation, pitch torque initially pushed positive (head tilting downwards, as defined in Fig. 1A).

Stimulated wingstrokes showed peak changes of 4 mN m or more compared with the immediately preceding wingstroke (Fig. 4). These changes lessened over the course of the wingstroke. Changes in torque were notably larger when the DLM was activated in early-wingstroke phases of less than 0.25. As a built-in control for the realism of evoked MAPs, for all individuals these changes due to stimulation progressively lessened as evoked DLM timing approached naturalistic timing around 40–50% of wingstroke phase.

In summary, changing the relative timing between the activation of downstroke and upstroke flight power muscles affects both mean pitch torque (Fig. 4C) and the deviation of mean pitch torque from normal dynamics (Fig. 4D). Altered DLM timing demonstrated consistent changes to within-wingstroke pitch torque dynamics in the form of a large oscillation in pitch torque following DLM spike phase, with the amplitude of this oscillation increasing the farther the DLM was evoked to spike relative to naturalistic timing. These features of causal manipulation of DLM timing, however, are purely

Journal of Experimental Biology (2024) 227, jeb246840. doi:10.1242/jeb.246840

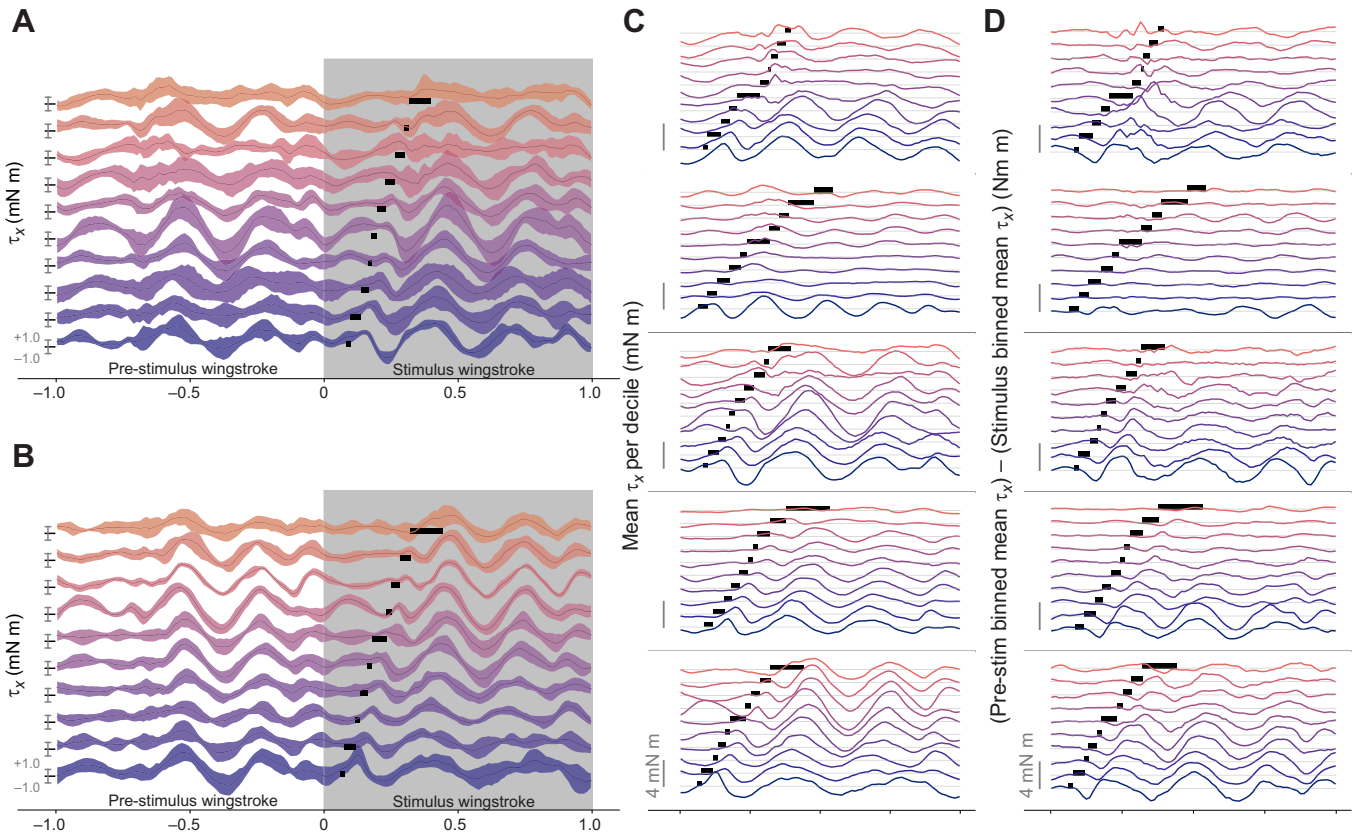

Fig. 4. Qualitative features of stimulation visible in mean pitch torque waveforms binned by decile of stimulation phase. (A,B) Mean±1 standard deviation (s.d.) of time-varying pitch torque (τ_x) in the wingstrokes before, during and after stimulation for two example individuals, binned by decile of stimulation phase. Each binned mean±s.d. trace contains the same number of pitch torque traces. Bars in the stimulus wingstroke indicate the minimum to maximum range of phases during which the stimulus was applied for each binned group. Axes on the left of each trace indicate where pitch torque is 0, +1 and −1 mN m for each group. (C) Plots following A and B for all individuals, but showing only mean pitch torque for only the stimulation wingstroke. (D) Difference in mean pitch torque during stimulated wingstroke compared with pre-stimulation wingstroke. At each phase the difference $\tau_{x,pre}-\tau_{x,stim}$ is taken, so this plot indicates the deviation from the undisturbed, pre-stimulation pitch torque profile. Scale bars in C and D indicate 4 mN m for each individual, light gray lines indicate 0 mN m for each decile.

qualitative. Surrounded by natural variation in pitch torque and the underlying motor program, features of pitch torque directly tied to evoked DLM timing are difficult to quantify without some form of directed feature extraction.

CCA features demonstrate power muscles have mechanically relevant influence on pitch torque

To determine whether the power muscles have a controllable influence on pitch, and how much variation in pitch torque is causally attributable to power muscle timing, requires quantifying the specific features of pitch torque associated with DLM phase. CCA was applied to extract these features of pitch torque which maximally covaried with evoked changes in DLM phase (Fig. 5). CCA features picked out the same observed trend in Fig. 4, with the main cyclic oscillations of pitch torque shifting earlier in phase as the DLM was induced to spike earlier. Notably, even a non-linear kernel CCA extracted similar features (Figs S1 and S2) with only slightly higher variance explained, indicating that the underlying relationship between induced DLM phase and pitch torque is robust and well approximated by linear CCA.

If DLM phase has a causal, controllable effect on body pitch, the angular impulse (change in angular momentum) in the stimulation wingstroke should vary significantly with DLM phase. The angular impulse in pitch imparted by reconstructed CCA features (Eqn 2) varied linearly with DLM phase (Fig. 6A) with a statistically significant positive slope across individuals ($P<10^{-3}$). A significant slope is unsurprising, as CCA inherently finds features which maximally correlate with evoked DLM timing. CCA, however, is agnostic to the directionality of this relationship, so a positive slope indicates the maximally correlated relationship between these two variables is positive. Such a positive relationship indicates a more negative angular momentum (more nose-up pitch) is linearly associated with a greater interval between the DLM and DVM, matching observations of the correlational experiment where greater t_{DVM}–t_{DLM} was associated with pitching up (Fig. 3E).

To assess the behavioral relevance of these pitch torques, we divided angular impulse by pitch moment of inertia I_{yy}, giving the effective change in pitch angular velocity Δω over a wingstroke (Eqn 3). The change in pitch angular velocity over a wingstroke due to reconstructed features increased by at least 400 deg s^{-1} between early and late DLM phase in every individual (Fig. 6B). For a typical 50 ms wingstroke, 400 deg s^{-1} corresponds to a change of at least 20 deg in body pitch angle over a single wingstroke, a relevant amount of change from a flight control perspective. Pitch angular velocity of 400 deg s^{-1} is also well in line with free-flight pitching maneuvers, where pitch angular velocities observed to vary between −500 to +500 deg s^{-1} in *Manduca* (Cheng et al., 2011).

Journal of Experimental Biology (2024) 227, jeb246840. doi:10.1242/jeb.246840

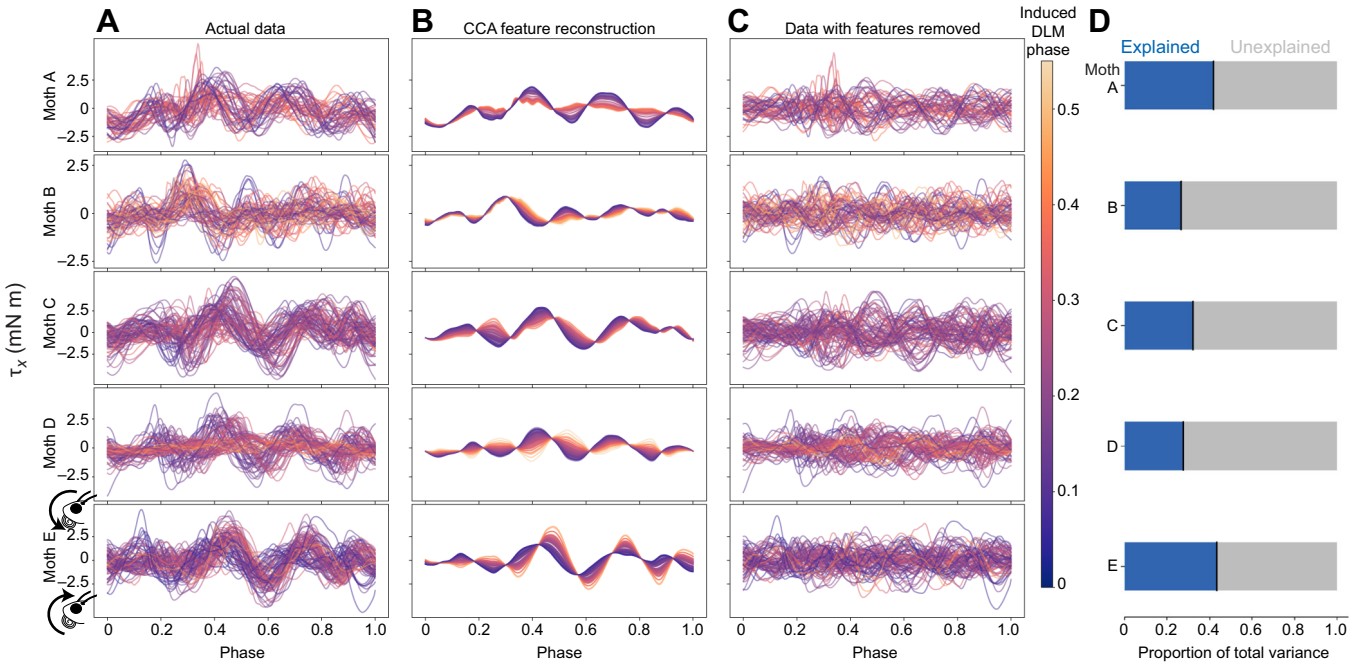

Fig. 5. Features of pitch torque which covary with evoked DLM timing show consistent phase shift in pitch torque. (A) Actual data of pitch torque (τ_x) in stimulation wingstroke, colored by evoked DLM phase on the same scale as in Fig. 4A–D. Inset diagrams of moth heads on the bottom row indicate pitch sign convention. (B) CCA feature reconstructions of pitch torque in stimulation wingstroke, colored by evoked DLM phase. Reconstructions were generated using Eqn 1 followed by removal of *z*-scoring. (C) Raw data with CCA feature reconstructions subtracted, leaving only variance in pitch torque signal unexplained by CCA features. (D) Proportion of total variance explained by CCA feature reconstructions (blue, left) versus unexplained (gray, right).

While it is clear that the features of pitch torque driven by the DLM demonstrate a causal and mechanically relevant influence on body pitch, there was a notable amount of unexplained variance of pitch torque in the stimulation wingstroke (Fig. 5D). On average across individuals, 64.5±6.7% of the variance of pitch torque was not explained by a linear feature of evoked DLM phase. Similarly, the magnitude of pitch angular impulse due to CCA features was far smaller than overall pitch angular impulse (Fig. 6A). Though the angular impulse of CCA features alone had a statistically significant linear relationship with induced DLM timing, no such relationship was detectable between induced DLM timing and total angular impulse, or between induced DLM phase and any wingstroke-averaged torques (Table S1, Fig. S3). Altogether, this indicates that the degree to which muscles other than the DLM influence pitch torque is high, and the DLM does not control pitch in isolation.

DISCUSSION

Power muscles contribute to pitch control in hawkmoth flight

The two experiments of this paper present correlational and causal evidence which supports the hypothesis that bilaterally symmetric changes in DLM spike timing alter body pitch. Greater time between the DLMs and DVMs leads to upwards pitch, and less time leads to downwards pitch. In the first experiment, pitch turns were visually induced and verified to produce separated responses in mean-centered torques only about the pitch axis (Fig. 1), and decreases in the phase between the DLM and DVM were observed in pitch down turns compared with pitch up (Fig. 3). This correlational finding was corroborated through causal manipulation of DLM–DVM timing (Fig. 2), where features of pitch torque that covaried with evoked DLM timing shifted towards downwards mean pitch as the time between the DLM and DVM decreased (Fig. 5). Bilaterally asymmetric power muscle timing has been linked to control of yaw turns in flies and hawkmoths (Lehmann et al., 2013; Sponberg and Daniel, 2012; Tu and Daniel, 2004), and while in flies DLM motor neuron firing rate can modulate symmetric power and wingstroke amplitude (Gordon and Dickinson, 2006), to date no studies have shown symmetric power muscle timing causally affecting pitch. This is a particularly relevant finding, then, as pitch is part of an inherently unstable dynamic mode, and requires active control on relatively short time scales of the order of ∼45 ms for *Manduca* (Ristroph et al., 2013), similar to the duration of a typical wingbeat of ∼50 ms.

The ability for the indirect flight muscles to control pitch does not preclude known contributions from direct steering muscles in species including *Drosophila* (Whitehead et al., 2015, 2022) and *Manduca* (Ando and Kanzaki, 2004). This is consistent with induced changes in DLM timing relative to DVMs producing consistent pitch torque features, but the variance explained by these features being relatively low (Fig. 5D) and the angular impulse of these features, while relevant, presenting as small compared with overall impulse (Fig. 6).

A smaller influence of the indirect power muscles on pitch, however, is still behaviorally relevant. Despite often being much smaller than total pitch impulse, the impulse from CCA features was large enough in all individuals to cause 400 deg s^{-1} or more change in pitch angular velocity over single wingstrokes (Fig. 6). Both the amount of pitch imparted by CCA features and the ranges of DLM timing required to do so are highly plausible in free flight. The observed 400 deg s^{-1} pitch velocity change closely matches the ±500 deg s^{-1} pitch velocity observed in *Manduca* free flight (Cheng et al., 2011), and in natural, unmanipulated wingstrokes the DLM spikes between 20% and 55% of the wingstroke phase (Putney et al., 2019). So even though the most pronounced effects of causally manipulating DLM phase on pitch torque occurred in earlier phases near 20–30% (Fig. 4D), these phases are consistent

Journal of Experimental Biology (2024) 227, jeb246840. doi:10.1242/jeb.246840

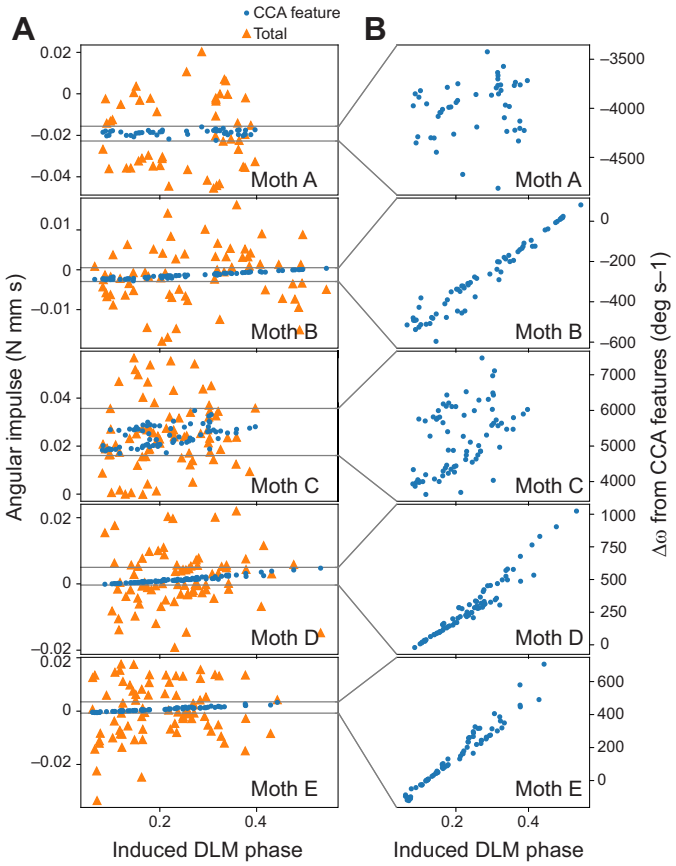

Fig. 6. CCA features produce mechanically relevant levels of angular impulse in pitch. (A) Overall angular impulse from pitch torque (orange triangles; Fig. 5A) and angular impulse from just CCA feature reconstructions of pitch torque associated with DLM phase (blue circles; Fig. 5B) for each individual moth. (B) Pitch angular velocity change (Δω) due to angular impulse from CCA feature reconstructions.

with the natural timing range of the DLM. Thus, while the overall effects of the DLM may only explain ∼40% of the variation in pitch torque, this is a relevant amount of variation when it comes to controlling the unstable mode of pitch as the observed effects on pitch from the DLM are reasonably expected to occur in natural free flight.

Possible mechanisms for power muscles to modulate pitch

For a flapping wing animal such as an insect, there are four possible ways to produce and modulate body pitch torque: (1) move the location of the body COM relative to the wing COP to change the moment arm on which aerodynamic forces are applied (e.g. abdominal flexion); (2) modify the wingstroke-averaged or time-varying location of the COP in relation to the COM by altering wing kinematics (e.g. changing wing sweep angle); (3) alter wing kinematics to generate inertial moments on the COM; and (4) change the within-wingstroke aerodynamic forces produced by the wings (e.g. changing the duration of the downstroke and upstroke to exploit moment asymmetries between the two phases of the wingstroke). Note that these mechanisms all interact and are not independent; varying wing kinematics will always change both aerodynamic and inertial forces. This means that of these four mechanisms, only the first (moving the COM relative to the COP) is unavailable to the indirect power muscles, as they are only able to alter wing kinematics.

Narrowing these four possible mechanisms down further, producing purely inertial moments is an unlikely mechanism to be used in isolation. For indirect power muscles, then, the most plausible kinematic mechanisms to exert pitch control are either by changing time-varying wing forces or by moving the COP, both of which have been observed in hawkmoths. In freely flying hawkmoths, wing pitch angle, or the spatial average rotation of the wing about its base-to-tip axis, correlates directly with body pitching movements (Cheng et al., 2011). As confirmed by a model robotic flapping wing, varying wing pitch angle had a clear effect of altering time-varying wing forces by altering the wing angle of attack. Increase the wingstroke mean wing pitch angle, and the angle of attack is increased during downstroke and decreased during upstroke, leading to a net nose-up pitching moment (Cheng et al., 2011). While the power muscles of hummingbirds do generate a wing pitch torque (Agrawal et al., 2022), it is unclear how hawkmoth power muscles could alter wing pitch angle, as the indirect hawkmoth power muscles have potentially less diverse effects on the wing's motion, primarily acting only on the stroke plane (Kammer, 1985). Instead, in hawkmoths, pitch angle is a kinematic quantity thought to be primarily controlled by direct steering muscles such as the 3rd axillary muscle (Ando and Kanzaki, 2004; Rheuben and Kammer, 1987).

Moving the COP relative to the COM is a more likely method for indirect power muscles to modulate pitch. Tilting of the wingstroke plane, while a well-established option for controlling pitch (Taylor and Thomas, 2002; Willmott and Ellington, 1997; Zanker, 1988), is less plausible for power muscles which produce motion along the major stroke plane, and for which there is little evidence of a mechanism for them to alter the angle of this plane. But altering the wing sweep, or angle the wings trace along the wingstroke plane, is a very plausible mechanism for power muscles to alter body pitch. Free flying hawkmoths are already known to asymmetrically reduce the ventral sweep amplitude to produce pitching moments (Willmott and Ellington, 1997). The timing of the DLM and DVM alters the wingstroke amplitude and sweep angle along the stroke plane from wingstroke to wingstroke in hawkmoths (Ando and Kanzaki, 2016; Wang et al., 2008). Adjusting the wingstroke sweep angle would change the COP location relative to the COM, allowing power muscles to control both pitch torques. Dipterans have long been known to use this mechanism of changing stroke amplitude to drive pitch control by shifting the wingstroke mean aerodynamic forces at the COP (Dickinson, 1999; Hollick, 1940; Nalbach and Hengstenberg, 1994; Taylor, 2001; Whitehead et al., 2015, 2022). For these reasons, of the possible kinematics mechanisms listed, we find it most likely that power muscles in *M. sexta* exert pitch control authority through wingstroke amplitude and sweep angle.

It is important to note that all data in this study come from dorsally tethered moths. Tethering decreases wingstroke frequency of hawkmoths (Ando and Kanzaki, 2004), and is known to have an impact on kinematics (Fry et al., 2005), particularly on wing sweep and wingstroke amplitude. It is possible that the exact nature and amount of effect observed in pitch torque from altering DLM phase might differ in free flight. However, the repeatability of the DLM's effect on pitch torque across individuals and the tendency of individual moths to have very different wing kinematics suggest the relationship between DLM phase and pitch torque is robust to the unperturbed state of wing kinematics.

That being said, it is clear the DLM does not act alone in controlling pitch, and that any pitch control potential from power muscles happens in concert with the control potential of direct steering muscles. The kinematic mechanisms we implicate for

indirect power muscle control of wing sweep and wingstroke amplitude are already well known to be affected by steering muscles. In flies, the 1st and 2nd basalar muscles contribute to the control of wing sweep and wingstroke amplitude on short time scales (Balint and Dickinson, 2001; Heide and Götz, 1996; Lehmann and Götz, 1996; Lindsay et al., 2017; Tu and Dickinson, 1996; Whitehead et al., 2015, 2022). Especially for synchronous flying insects such as hawkmoths, the direct flight musculature is always active (Kammer, 1971; Putney et al., 2019) and has an undeniable, constant role in any flight control. Our results demonstrate that the indirect power muscles have some control potential on body pitch, but this control potential can only occur in the context of the rest of the motor program and flight musculature.

Precisely changing the timing of one power muscle does not precisely determine a turn

Of important note is the relatively high amount of unexplained variance left after removal of CCA features (Fig. 5C,D; 64.5±6.7% across individuals). While CCA does not extract features which maximize variance in a dataset, only seeking features which maximize covariance between pitch torque and evoked DLM timing, the large amount of pitch torque signal unexplained by evoked DLM timing leaves an interesting implication. Despite the DLM being the largest muscle in *M. sexta*, large changes to DLM timing did not lead to large changes in tethered flight dynamics. Stated differently, the timing of one power muscle alone does not produce a turn.

Our results put a precise understanding on where, between the two extremes of functionally overlapping and functionally separated, the hawkmoth flight power musculature falls. By using causal electrical stimulation in concert with dual dimensionality reduction, we directly measured the degree to which a specific behavioral output, pitch torque, is driven by the control potential of a single pair of muscles, the DLMs. The DLMs do exert a measurable control potential on pitch torque sufficient to produce pitch turns (Figs 4D and 6B), and have a consistent within-wingstroke signature on pitch torque (Figs 4 and 5). But the features of pitch torque associated with the timing of the DLMs fail to explain most of the variation in pitch torque (Fig. 5D) and poorly describe quantities on the time scale of the entire wingstroke, such as pitch angular impulse (Fig. 6A) or any wingstroke-averaged torques (Fig. S3). These results show that in controlling body pitch, at least some subset of the flight musculature must be coordinated to produce a pitch turn. Even if all the flight muscles have fully separate and non-overlapping kinematic functions, to produce the results observed, these muscles must have some functional overlap in pitch torque.

This fits well with prior results in hawkmoths and other flying insects, where measurable functional overlap and interactions between muscles means that adequate descriptions of behavior require the activity of many coordinated muscles. In flies, the 1st and 2nd basalar muscles are frequently correlated to stroke amplitude (Balint and Dickinson, 2001; Heide and Götz, 1996; Lehmann and Götz, 1996; Lindsay et al., 2017; Whitehead et al., 2015, 2022). But even these two muscles are known to have interacting kinematic effects (Dickinson and Tu, 1997; Tu and Dickinson, 1994, 1996), and the activity of at least 8 of 12 steering muscles is required to describe any more than 30% of the variance of just wing stroke amplitude (Lindsay et al., 2017). In hawkmoths, activity from four or more muscles is needed to decode just the type of turn being performed with more than 90% accuracy (Putney et al., 2021 preprint). Similarly, redundant global information in spike timing has been observed across the entire flight motor program (Putney et al., 2019), suggesting functional coordination such that individual muscles are controlled in the context of the rest of the motor program.

Our results also provide a causal test of the temporal precision that has been estimated from information theoretic analysis of the hawkmoth flight motor program (Putney et al., 2019, 2023b). Moths were not tuned or directly cued to any particular maneuver other than wing flapping, and thus changes to DLM timing were applied across a distribution of locomotor coordination states. Precise changes in DLM timing did lead to precise changes in the CCA feature space (Fig. 6B), but these small changes were typically only a portion of the variation in the rest of the motor program (Fig. 6A). Thus, precision is relative to coordination. While the spike timing of a muscle may describe the yaw torque of a hawkmoth to a sub-millisecond scale (Putney et al., 2023b), this is only in the context of the rest of the motor program also aiming to produce that yaw torque. When muscles functionally overlap to control an outcome such as pitch or yaw torque, the specific timing of one muscle is context dependent, with an impact which can be cancelled out by other muscles.

Overall, then, our results underline the importance of coordination in flight musculature to produce controlled flight. While kinematic or behavioral outcomes can be causally attributed to the spike timing of individual muscles, there is enough functional overlap between muscles in the flight motor program to make the effects of muscle spike timing context dependent. Even the largest and most powerful muscles in a hawkmoth have only so much explanatory power when manipulated outside of the coordinated activity of all other muscles.

Acknowledgements

We would like to acknowledge the other members of the agile systems lab for their discussions, support and feedback.

Competing interests

The authors declare no competing or financial interests.

Author contributions

Conceptualization: L.J.W., J.P., S.S.; Methodology: L.J.W., J.P.; Software: L.J.W.; Formal analysis: L.J.W., J.P.; Investigation: L.J.W., J.P.; Resources: S.S.; Data curation: L.J.W., J.P.; Writing - original draft: L.J.W.; Writing - review & editing: L.J.W., J.P., S.S.; Visualization: L.J.W., J.P.; Supervision: S.S.; Project administration: S.S.; Funding acquisition: S.S.

Funding

This work was supported by Air Force Office of Scientific Research grants FA9550-19-1-0396 and FA955022-1-0315, a Klingenstein-Simons Fellowship Award in Neuroscience, and a Dunn Family Endowment to S.S. Open Access funding provided by Georgia Institute of Technology. Deposited in PMC for immediate release.

Data availability

High-amplitude optomotor-induced turns data are available from Dryad (Putney et al., 2023a; https://doi.org/10.5061/dryad.zgmsbccnt), as is electrical stimulation experiment data (Wood et al., 2024; https://doi.org/10.5061/dryad.76hdr7t4f). Code for optomotor turns analysis is available upon request; code for electrical stimulation experiment analysis is available from GitHub (https://github.com/LeoJW/stimPitchAnalysis).

ECR Spotlight

This article has an associated ECR Spotlight interview with Leo Wood.

References

Agrawal, S., Tobalske, B. W., Anwar, Z., Luo, H., Hedrick, T. L. and Cheng, B. (2022). Musculoskeletal wing-actuation model of hummingbirds predicts diverse effects of primary flight muscles in hovering flight. *Proc. R. Soc. B* **289**, 20222076. doi:10.1098/rspb.2022.2076

Ando, N. and Kanzaki, R. (2004). Changing motor patterns of the 3rd axillary muscle activities associated with longitudinal control in freely flying hawkmoths. *Zoolog. Sci.* **21**, 123-130. doi:10.2108/zsj.21.123

Ando, N. and Kanzaki, R. (2016). Flexibility and control of thorax deformation during hawkmoth flight. *Biol. Lett.* **12**, 20150733. doi:10.1098/rsbl.2015.0733
Balint, C. N. and Dickinson, M. H. (2001). The correlation between wing kinematics and steering muscle activity in the blowfly *Calliphora vicina*. *J. Exp. Biol.* **204**, 4213-4226. doi:10.1242/jeb.204.24.4213
Balint, C. N. and Dickinson, M. H. (2004). Neuromuscular control of aerodynamic forces and moments in the blowfly, *Calliphora vicina*. *J. Exp. Biol.* **207**, 3813-3838. doi:10.1242/jeb.01229
Cheng, B., Deng, X. and Hedrick, T. L. (2011). The mechanics and control of pitching manoeuvres in a freely flying hawkmoth (*Manduca sexta*). *J. Exp. Biol.* **214**, 4092-4106. doi:10.1242/jeb.062760
Dickinson, M. H. (1999). Haltere–mediated equilibrium reflexes of the fruit fly, drosophila melanogaster. *Philos. Trans. R. Soc. Lond. B Biol. Sci.* **354**, 903-916. doi:10.1098/rstb.1999.0442
Dickinson, M. H. and Tu, M. S. (1997). The function of dipteran flight muscle. *Comp. Biochem. Physiol. A Physiol.* **116**, 223-238. doi:10.1016/S0300-9629(96)00162-4
Eaton, J. L. (1988). *Lepidopteran Anatomy.* John Wiley & Sons Limited.
Fernández, M. J., Springthorpe, D. and Hedrick, T. L. (2012). Neuromuscular and biomechanical compensation for wing asymmetry in insect hovering flight. *J. Exp. Biol.* **215**, 3631-3638. doi:10.1242/jeb.073627
Fry, S. N., Sayaman, R. and Dickinson, M. H. (2005). The aerodynamics of hovering flight in *Drosophila*. *J. Exp. Biol.* **208**, 2303-2318. doi:10.1242/jeb.01612
Frye, M. A. (2001). Effects of stretch receptor ablation on the optomotor control of lift in the hawkmoth *Manduca sexta*. *J. Exp. Biol.* **204**, 3683-3691. doi:10.1242/jeb.204.21.3683
Gordon, S. and Dickinson, M. H. (2006). Role of calcium in the regulation of mechanical power in insect flight. *Proc. Natl Acad. Sci. USA* **103**, 4311-4315. doi:10.1073/pnas.0510109103
Hedenström, A. (2014). How insect flight steering muscles work. *PLoS Biol.* **12**, e1001822. doi:10.1371/journal.pbio.1001822
Hedrick, T. L. and Daniel, T. L. (2006). Flight control in the hawkmoth *Manduca sexta*: the inverse problem of hovering. *J. Exp. Biol.* **209**, 3114-3130. doi:10.1242/jeb.02363
Hedrick, T. L., Martínez-Blat, J. and Goodman, M. J. (2017). Flight motor modulation with speed in the hawkmoth *Manduca sexta*. *J. Insect Physiol.* **96**, 115-121. doi:10.1016/j.jinsphys.2016.10.003
Heide, G. and Götz, K. G. (1996). Optomotor control of course and altitude in drosophila melanogaster is correlated with distinct activities of at least three pairs of flight steering muscles. *J. Exp. Biol.* **199**, 1711-1726. doi:10.1242/jeb.199.8.1711
Hill, D. N., Curtis, J. C., Moore, J. D. and Kleinfeld, D. (2011). Primary motor cortex reports efferent control of vibrissa motion on multiple timescales. *Neuron* **72**, 344-356. doi:10.1016/j.neuron.2011.09.020
Hinterwirth, A. J. and Daniel, T. L. (2010). Antennae in the hawkmoth *Manduca sexta* (Lepidoptera, Sphingidae) mediate abdominal flexion in response to mechanical stimuli. *J. Comp. Physiol. A* **196**, 947-956. doi:10.1007/s00359-010-0578-5
Hollick, F. S. J. (1940). The flight of the dipterous fly *Muscina stabulans* Fallén. *Philos. Trans. R. Soc. Lond. B Biol. Sci.* **230**, 357-390.
Jankauski, M., Daniel, T. L. and Shen, I. Y. (2017). Asymmetries in wing inertial and aerodynamic torques contribute to steering in flying insects. *Bioinspir. Biomim.* **12**, 046001. doi:10.1088/1748-3190/aa714e
Kammer, A. E. (1985). Flying. In *Comprehensive Insect Physiology, Biochemistry and Pharmacology (ed.* G. A. Kerkut and L. I. Gilbert et al.), pp. 491-552. Oxford: Pergamon.
Kammer, A. E. (1971). The motor output during turning flight in a hawkmoth, *Manduca sexta*. *J. Insect Physiol.* **17**, 1073-1086. doi:10.1016/0022-1910(71)90011-4
Kim, J.-K. and Han, J.-H. (2014). A multibody approach for 6-dof flight dynamics and stability analysis of the hawkmoth *Manduca sexta*. *Bioinspir. Biomim.* **9**, 016011. doi:10.1088/1748-3182/9/1/016011
Kim, J.-K., Han, J.-S., Lee, J.-S. and Han, J.-H. (2015). Hovering and forward flight of the hawkmoth *Manduca sexta*: trim search and 6-dof dynamic stability characterization. *Bioinspir. Biomim.* **10**, 056012. doi:10.1088/1748-3190/10/5/056012
Kutch, J. J. and Valero-Cuevas, F. J. (2011). Muscle redundancy does not imply robustness to muscle dysfunction. *J. Biomech.* **44**, 1264-1270. doi:10.1016/j.jbiomech.2011.02.014
Le, V., Cellini, B., Schilder, R. and Mongeau, J.-M. (2023). Hawkmoths regulate flight torques with their abdomen for yaw control. *J. Exp. Biol.* **226**, jeb245063. doi:10.1242/jeb.245063
Lehmann, F. O. and Götz, K. G. (1996). Activation phase ensures kinematic efficacy in flight-steering muscles of *Drosophila melanogaster*. *J. Comp. Physiol. A* **179**, 311-322. doi:10.1007/BF00194985
Lehmann, F.-O., Skandalis, D. A. and Berthé, R. (2013). Calcium signalling indicates bilateral power balancing in the drosophila flight muscle during manoeuvring flight. *J. R. Soc. Interface* **10**, 20121050. doi:10.1098/rsif.2012.1050
Lindsay, T., Sustar, A. and Dickinson, M. (2017). The function and organization of the motor system controlling flight maneuvers in flies. *Curr. Biol.* **27**, 345-358. doi:10.1016/j.cub.2016.12.018
Melis, J. M., Siwanowicz, I. and Dickinson, M. H. (2024). Machine learning reveals the control mechanics of an insect wing hinge. *Nature* **628**, 795-803. doi:10.1038/s41586-024-07293-4
Nalbach, G. and Hengstenberg, R. (1994). The halteres of the blowfly calliphora: Ii. three-dimensional organization of compensatory reactions to real and simulated rotations. *J. Comp. Physiol. A* **175**, 695-708. doi:10.1007/BF00191842
Pedregosa, F., Varoquaux, G., Gramfort, A., Michel, V., Thirion, B., Grisel, O., Blondel, M., Prettenhofer, P., Weiss, R., Dubourg, V. et al. (2011). Scikit-learn: Machine learning in Python. *J. Mach. Learn. Res.* **12**, 2825-2830.
Putney, J., Conn, R. and Sponberg, S. (2019). Precise timing is ubiquitous, consistent, and coordinated across a comprehensive, spike-resolved flight motor program. *Proc. Natl Acad. Sci. USA* **116**, 26951-26960. doi:10.1073/pnas.1907513116
Putney, J., Angjelichinoski, M., Ravier, R., Ferrari, S., Tarokh, V. and Sponberg, S. (2021). Consistent coordination patterns provide near perfect behavior decoding in a comprehensive motor program for insect flight. *bioRxiv*. doi:10.1101/2021.07.13.452211
Putney, J., Anjelichinoski, M., Ravier, R., Ferrari, S., Tarokh, V. and Sponberg, S. (2023a). Consistent coordination patterns provide near perfect behavior decoding in a comprehensive motor program for insect flight. *Dryad, Dataset*. doi:10.5061/dryad.zgmsbccnt
Putney, J., Niebur, T., Wood, L., Conn, R. and Sponberg, S. (2023b). An information theoretic method to resolve millisecond-scale spike timing precision in a comprehensive motor program. *PLoS Comput. Biol.* **19**, e1011170. doi:10.1371/journal.pcbi.1011170
Revzen, S. and Guckenheimer, J. M. (2008). Estimating the phase of synchronized oscillators. *Phys. Rev. E* **78**, 051907. doi:10.1103/PhysRevE.78.051907
Rheuben, M. B. (1985). Quantitative comparison of the structural features of slow and fast neuromuscular junctions in *Manduca*. *J. Neurosci.* **5**, 1704-1716. doi:10.1523/JNEUROSCI.05-07-01704.1985
Rheuben, M. B. and Kammer, A. E. (1987). Structure and innervation of the third axillary muscle of *Manduca* relative to its role in turning flight. *J. Exp. Biol.* **131**, 373-402. doi:10.1242/jeb.131.1.373
Ristroph, L., Ristroph, G., Morozova, S., Bergou, A. J., Chang, S., Guckenheimer, J., Jane Wang, Z. and Cohen, I. (2013). Active and passive stabilization of body pitch in insect flight. *J. R. Soc. Interface* **10**, 20130237. doi:10.1098/rsif.2013.0237
Sadaf, S., Venkateswara Reddy, O., Sane, S. P. and Hasan, G. (2015). Neural control of wing coordination in flies. *Curr. Biol.* **25**, 80-86. doi:10.1016/j.cub.2014.10.069
Sato, H. and Maharbiz, M. M. (2010). Recent developments in the remote radio control of insect flight. *Front. Neurosci.* **4**, 199. doi:10.3389/fnins.2010.00199
Sato, H., Vo Doan, T. T., Kolev, S., Huynh, N. A., Zhang, C., Massey, T. L., Van Kleef, J., Ikeda, K., Abbeel, P. and Maharbiz, M. M. (2015). Deciphering the role of a coleopteran steering muscle via free flight stimulation. *Curr. Biol.* **25**, 798-803. doi:10.1016/j.cub.2015.01.051
Sober, S. J., Sponberg, S., Nemenman, I. and Ting, L. H. (2018). Millisecond spike timing codes for motor control. *Trends Neurosci.* **41**, 644-648. doi:10.1016/j.tins.2018.08.010
Sponberg, S. and Daniel, T. L. (2012). Abdicating power for control: a precision timing strategy to modulate function of flight power muscles. *Proc. R. Soc. B* **279**, 3958-3966. doi:10.1098/rspb.2012.1085
Sponberg, S., Spence, A. J., Mullens, C. H. and Full, R. J. (2011). A single muscle's multifunctional control potential of body dynamics for postural control and running. *Philos. Trans. R. Soc. B Biol. Sci.* **366**, 1592-1605. doi:10.1098/rstb.2010.0367
Sponberg, S., Daniel, T. L. and Fairhall, A. L. (2015a). Dual dimensionality reduction reveals independent encoding of motor features in a muscle synergy for insect flight control. *PLoS Comput. Biol.* **11**, e1004168. doi:10.1371/journal.pcbi.1004168
Sponberg, S., Dyhr, J. P., Hall, R. W. and Daniel, T. L. (2015b). Luminance-dependent visual processing enables moth flight in low light. *Science* **348**, 1245-1248. doi:10.1126/science.aaa3042
Springthorpe, D., Fernández, M. J. and Hedrick, T. L. (2012). Neuromuscular control of free-flight yaw turns in the hawkmoth manduca sexta. *J. Exp. Biol.* **215**, 1766-1774. doi:10.1242/jeb.067355
Stöckl, A. L., O'Carroll, D. and Warrant, E. J. (2017). Higher-order neural processing tunes motion neurons to visual ecology in three species of hawkmoths. *Proc. R. Soc. B* **284**, 20170880. doi:10.1098/rspb.2017.0880
Taha, H. E., Kiani, M., Hedrick, T. L. and Greeter, J. S. (2020). Vibrational control: A hidden stabilization mechanism in insect flight. *Sci. Robot.* **5**, eabb1502. doi:10.1126/scirobotics.abb1502
Taylor, G. K. and Thomas, A. L. R. (2002). Animal flight dynamics ii. longitudinal stability in flapping flight. *J. Theor. Biol.* **214**, 351-370. doi:10.1006/jtbi.2001.2470
Taylor, G. K. (2001). Mechanics and aerodynamics of insect flight control. *Biol. Rev.* **76**, 449-471. doi:10.1017/S1464793101005759
Ting, L. H. (2007). Dimensional reduction in sensorimotor systems: a framework for understanding muscle coordination of posture. *Prog. Brain Res.* **165**, 299-321. doi:10.1016/S0079-6123(06)65019-X

Tsang, W. M., Stone, A. L., Aldworth, Z. N., Hildebrand, J. G., Daniel, T. L., Akinwande, A. I. and Voldman, J. (2010). Flexible split-ring electrode for insect flight biasing using multisite neural stimulation. *IEEE Trans. Biomed. Eng.* **57**, 1757-1764. doi:10.1109/TBME.2010.2041778

Tu, M. S. and Daniel, T. L. (2004). Submaximal power output from the dorsolongitudinal flight muscles of the hawkmoth *Manduca sexta*. *J. Exp. Biol.* **207**, 4651-4662. doi:10.1242/jeb.01321

Tu, M. S. and Dickinson, M. (1994). Modulation of negative work output from a steering muscle of the blowfly *Calliphora vicina*. *J. Exp. Biol.* **192**, 207-224. doi:10.1242/jeb.192.1.207

Tu, M. S. and Dickinson, M. H. (1996). The control of wing kinematics by two steering muscles of the blowfly (*Calliphora vicina*). *J. Comp. Physiol. A* **178**, 813-830.

Usherwood, P. N. R. (1962). The nature of 'slow'and 'fast'contractions in the coxal muscles of the cockroach. *J. Insect Physiol.* **8**, 31-52. doi:10.1016/0022-1910(62)90052-5

Valero-Cuevas, F. J. (2009). A mathematical approach to the mechanical capabilities of limbs and fingers. *Adv. Exp. Med. Biol.* **629**, 619-633. doi:10.1007/978-0-387-77064-2_33

Vazquez, R. J. (1995). Functional anatomy of the pigeon hand (*Columba livia*): a muscle stimulation study. *J. Morphol.* **226**, 33-45. doi:10.1002/jmor.1052260104

Wang, H., Ando, N. and Kanzaki, R. (2008). Active control of free flight manoeuvres in a hawkmoth, *Agrius Convolvuli*. *J. Exp. Biol.* **211**, 423-432. doi:10.1242/jeb.011791

Wegelin, J. A. (2000). *A survey of partial least squares (pls) methods, with emphasis on the two-block case*. Technical Report 371. Department of Statistics, University of Washington. https://stat.uw.edu/research/tech-reports/survey-partial-least-squares-pls-methods-emphasis-two-block-case

Whitehead, S. C., Beatus, T., Canale, L. and Cohen, I. (2015). Pitch perfect: how fruit flies control their body pitch angle. *J. Exp. Biol.* **218**, 3508-3519. doi:10.1242/jeb.122622

Whitehead, S. C., Leone, S., Lindsay, T., Meiselman, M. R., Cowan, N. J., Dickinson, M. H., Yapici, N., Stern, D. L., Shirangi, T. and Cohen, I. (2022). Neuromuscular embodiment of feedback control elements in *Drosophila* flight. *Sci. Adv.* **8**, eabo7461. doi:10.1126/sciadv.abo7461

Willmott, A. P. and Ellington, C. P. (1997). The mechanics of flight in the hawkmoth *Manduca sexta*. i. Kinematics of hovering and forward flight. *J. Exp. Biol.* **200**, 2705-2722. doi:10.1242/jeb.200.21.2705

Windsor, S. P., Bomphrey, R. J. and Taylor, G. K. (2014). Vision-based flight control in the hawkmoth *Hyles lineata*. *J. R. Soc. Interface* **11**, 20130921. doi:10.1098/rsif.2013.0921

Wood, L., Putney, J. and Sponberg, S. (2024). Flight power muscles have a coordinated, causal role in controlling hawkmoth pitch turns. *Dryad, Dataset*. doi:10.5061/dryad.76hdr7t4f

Zanker, J. M. (1988). On the mechanism of speed and altitude control in *Drosophila melanogaster*. *Physiol. Entomol.* **13**, 351-361. doi:10.1111/j.1365-3032.1988.tb00485.x